Confinement factors and optical gain in subwavelength plasmonic resonators

A. V. Maslov and M. Miyawaki

Citation: Journal of Applied Physics **108**, 083105 (2010); doi: 10.1063/1.3490766
View online: http://dx.doi.org/10.1063/1.3490766
View Table of Contents: http://scitation.aip.org/content/aip/journal/jap/108/8?ver=pdfcov
Published by the AIP Publishing

Confinement factors and optical gain in subwavelength plasmonic resonators

A. V. Maslov[a] and M. Miyawaki
Optics Research Laboratory, Canon U.S.A., Inc., 9030 S. Rita Rd., Suite 302, Tucson, Arizona 85747, USA

(Received 6 May 2010; accepted 19 August 2010; published online 21 October 2010)

We define the confinement factor for a subwavelength resonator, present a simple approach to calculate it numerically, and demonstrate that by using a specific resonator based on a silver rod coated with active material. Unlike the common approach of using the profile of the resonant electromagnetic mode, our formulation relies on using the characteristic equation for the complex frequency with inclusion of damping due to Joule and radiative losses. This removes an arbitrariness related to the definition of the mode volume in subwavelength resonators. Our analysis of a coated silver rod suggests that there is an optimal value for the active region thickness. The confinement factors can be comparable to that in Fabry–Perot resonators, radiative losses are comparable or exceed Joule losses and the threshold gain is high. © *2010 American Institute of Physics*.
[doi:10.1063/1.3490766]

I. INTRODUCTION

The size of a laser is typically determined by the size of the optical cavity. In the past two decades, vertical-cavity surface-emitting and photonic-crystal lasers have been explored to reduce the cavity size. The miniaturization trend continues and the structures using plasmon resonances in metals[1–3] and the waveguiding in semiconductor nanowires[4,5] have attracted recent attention. Heat-assisted magnetic storage[6] and high-resolution printing are among many promising applications of nanolasers.

One of the key quantities characterizing a laser cavity is the ratio of the cavity mode gain and material gain. The material gain is determined by the external carrier injection. This ratio depends on the geometry and material composition. Its knowledge allows one to estimate the required pumping (injection) level and determine the threshold material gain if the losses are also known. Resonant structures can be optimized to increase this unitless ratio and compared against each other.

For the resonant structures based on finite-length waveguides (such as edge-emitting lasers), the ratio of the guided mode gain to the material gain is often referred to as the confinement factor for the waveguide. The development of subwavelength structures required some revisions in the applicability of the traditional language used by the semiconductor laser community to nanolasers.[7] In particular, due to a reduced group velocity of the strongly guided modes, waveguide confinement factors greater than unity can be obtained despite the fact that the active region occupies only a fraction of the waveguide mode.[7–10] These values for the confinement factor are significantly higher than for the typical edge-emitting lasers. Furthermore, the gain confinement factors are not equal to the fraction of the mode power in the active region as sometimes assumed in the literature.[8,11,12]

The confinement factors relevant for waveguides are not applicable to resonant structures which are not based on guided modes. Such structures include metal particles, rods, bow-tie antennae, etc., which are currently of great interest for subwavelength operation. The definition for the confinement factor based on mode profile distribution, similar to that for waveguides, suffers from the lack of a unique definition of the cavity volume based on the geometrical consideration due to the fact that the electromagnetic field extends beyond the surface of the resonator. Furthermore, the size of practically used subwavelength structures is not significantly smaller than the wavelength and therefore, the field components other than the spatially decaying near field must be accounted for. This calls for a clear definition of the confinement factor in order to compare the performance of various resonators.

The purpose of this paper is twofold. First, we introduce and discuss the confinement factor for subwavelength resonators that is a generalization of the presently used confinement factor for waveguides. Second, we demonstrate its calculation by solving the complex characteristic equation for a specific resonator. As an example, we use a silver rod surrounded by gain medium. We use experimental values of the dielectric constant of silver that allows us to obtain results relevant to experiments. Unlike most of the works that treat various metal structures as resonators excited by plane waves[13] or dipole sources, we use the characteristic equation for the modes without explicitly assuming any incident radiation. The characteristic equation gives the frequency and decay rate for the lasing modes.

II. DEFINITION OF CONFINEMENT FACTOR AND ITS CALCULATION USING FIELD DISTRIBUTION

We start by defining the confinement factor. Let us take a resonator which is characterized by a mode oscillating at frequency ω with the real electric field

$$\mathbf{E}(\mathbf{r}) = A(t)\tilde{\mathbf{E}}(\mathbf{r})e^{-i\omega t} + \text{c.c.}, \quad (1)$$

[a]Electronic mail: amaslov@cusa.canon.com.

where $\tilde{\mathbf{E}}(\mathbf{r})$ is the complex mode profile and c.c. stands for complex conjugate. The normalization of the mode field $\tilde{\mathbf{E}}(\mathbf{r})$ is not important for gain calculations. The mode $\tilde{\mathbf{E}}(\mathbf{r})$ describes a standing wave that is calculated in the absence of loss or gain. The effects of loss or gain are subsequently added as time-dependence of the amplitude $A(t)$ perturbatively. We assume that the resonator has an active (gain) region. The gain region is characterized by a dielectric constant with a small imaginary part $\varepsilon_g=\varepsilon_g'+i\varepsilon_g''$ and $|\varepsilon_g''| \ll \varepsilon_g'$. The imaginary part ε_g'' gives rise to a finite value of work performed by the currents in the gain region during one period $T=2\pi/\omega$. This work reduces the total energy of the resonator W_{tot} by ΔW_{tot}

$$\frac{\Delta W_{\text{tot}}}{T} = |A|^2 \frac{\omega}{2\pi} \int_{\text{g.r.}} d\mathbf{r} \varepsilon_g'' |\tilde{\mathbf{E}}(\mathbf{r})|^2, \tag{2}$$

where the integral is taken over the gain region (g.r.). We keep all formulas in the Gaussian units. The total energy W_{tot} is calculated by integrating the energy density and includes the contributions from the electromagnetic fields as well as from the medium itself. Since explicit formulas for W_{tot} depend on specific models for the medium we do not give them here. Equation (2) gives the gain coefficient g (in the units of s^{-1}) defined as

$$\frac{dW_{\text{tot}}}{dt} = g W_{\text{tot}}, \tag{3}$$

$$g = -\frac{\omega}{2\pi W_0} \int_{\text{g.r.}} d\mathbf{r} \varepsilon_g'' |\tilde{\mathbf{E}}(\mathbf{r})|^2, \tag{4}$$

where W_0 is the energy for $A=1$ and $W_{\text{tot}}=|A|^2 W_0$. If ε_g'' is constant in space, we can further formally associate the integral in Eq. (4) with the time-averaged energy of the electric field

$$W_e = \int_{\text{g.r.}} d\mathbf{r} \frac{|\tilde{\mathbf{E}}(\mathbf{r})|^2}{4\pi} \tag{5}$$

and rewrite the gain in Eq. (4) as

$$g = -2\omega\varepsilon_g'' \frac{W_e}{W_0}. \tag{6}$$

Equation (5) describes only the energy of the electric field without the energy stored in the gain region in other forms, for example, as polarization. If dispersion in the gain region can be neglected, the energy associated with polarization can in principle be accounted for by multiplying Eq. (5) by ε_g' and then dividing Eq. (6) by the same factor. In the presence of dispersion such a procedure does not seem to be useful for gain calculations.

For waveguiding structures, the material gain is defined as the gain experienced by a plane wave in a uniform gain medium (in the units of cm^{-1}). This allows one to compare this gain against that in a specific guiding structure and define a unitless ratio of the two as the confinement factor. In the case of a resonator, it is more natural to compare its gain g against the gain g_0 inside a Fabry–Perot (FP) resonator filled with dielectric with complex dispersionless ε_g which has a small imaginary part. This allows us to introduce the gain confinement factor Γ as

$$g = \Gamma g_0. \tag{7}$$

Applying Eq. (6) to a FP resonator, we obtain

$$g_0 = -\omega' \frac{\varepsilon_g''}{\varepsilon_g'}. \tag{8}$$

And, therefore, Eq. (7) gives the confinement factor

$$\Gamma = -\frac{\varepsilon_g'}{2\pi W_0} \int_{\text{g.r.}} d\mathbf{r} |\tilde{\mathbf{E}}(\mathbf{r})|^2 = 2\frac{\varepsilon_g' W_e}{W_0}, \tag{9}$$

The FP gain g_0 is inversely proportional to the real part of the dielectric constant. This is simply due to the fact that only the electric field can provide gain and the presence of dielectric constant reduces the value of the electric field in favor of the polarization field. The confinement factor Γ for the FP resonator is defined as unity which is also consistent with Eq. (9).

III. CALCULATION OF CONFINEMENT FACTOR USING CHARACTERISTIC EQUATION FOR RESONATOR

When characterizing a resonator, one typically finds the resonant frequency first and then the mode profile. This is particularly true for complicated resonant structures in which the mode profile is not known. With the knowledge of the mode field, one then calculates the confinement factor using Eq. (9). Although the approach of calculating the confinement factor using the mode profile is quite reasonable it brings some difficulties, especially for subwavelength resonators. Indeed, it requires the knowledge of the total energy W_{tot} via integrating the field over the whole volume where the field exists. In the case of lasers based on waveguides with facets reflections (FP lasers) the integration is limited only to the volume of the resonator and neglects the field that leaks outside. This naturally leads to the unit value of the so-called longitudinal confinement factor.[7] However, for subwavelength structures, there is no well-defined boundary so defining the integrating volume becomes more difficult. In the limit of very small structures, one can use the quasistatic approximation to describe resonances. In this approximation, the fast decay of the near field allows one to extend integration to infinity and obtain a finite value for the energy.

However, the need of calculating mode profile and defining the integration volume can be avoided if one takes a different approach to obtain the gain and corresponding confinement factor. The application of such an approach to the calculation of the waveguide confinement factor using the properties of dispersion curve was described in Ref. 4. Here, we describe its application to resonators.

Let the resonant frequency be described by a known complex function $\omega(\varepsilon_g)=\omega'(\varepsilon_g)+i\omega''(\varepsilon_g)$. The corresponding fields behave as $\sim\exp(-i\omega t)$. The complex resonant frequency is related to representation (1) with the amplitude $A(t)=e^{\omega'' t}$. The real part (ω') is the position of the resonance, the imaginary part (ω'') is the width of the resonance. The

width determines the energy decay or gain rate, depending on its sign. The imaginary part can be separated into various contributions that arise from gain and radiative or Joule loss.

To describe the variation in the complex resonance due to change in ε_g, we expand the function $\omega(\varepsilon_g)$ near $\varepsilon_g=\varepsilon_g'$ assuming a small increment ε_g''

$$\omega(\varepsilon_g) \approx \omega(\varepsilon_g') + i\varepsilon_g'' \left.\frac{d\omega}{d\varepsilon_g}\right|_{\varepsilon_g=\varepsilon_g'}. \tag{10}$$

This expansion gives the following gain due to the presence of ε_g'':

$$g = 2\varepsilon_g'' \,\mathrm{Re}\left(\frac{d\omega}{d\varepsilon_g}\right). \tag{11}$$

Substituting the FP resonance condition $\omega(\varepsilon_g')=\omega' = \pi nc/(L\sqrt{\varepsilon_g'})$, with n an integer, into Eq. (10) gives

$$g_0 = 2\frac{d\omega'}{d\varepsilon_g}\varepsilon_g'' = -\omega'\frac{\varepsilon_g''}{\varepsilon_g'}, \tag{12}$$

which agrees with Eq. (8). Note that Eq. (12) is applicable not only to a FP resonator but to a wider range of resonators, for example, to the cavities wit perfectly conducting boundaries. As in Eq. (7), we introduce the confinement factor Γ for an arbitrary resonator as the ratio of modal g and FP g_0 gain. Using Eq. (11) and expression (8) we obtain

$$\Gamma \equiv \frac{g}{g_0} = -2\frac{\varepsilon_g'}{\omega'}\mathrm{Re}\left(\frac{d\omega}{d\varepsilon_g}\right). \tag{13}$$

Equation (13) not only defines Γ but also presents a way to calculate it using the derivative of the complex function $\omega(\varepsilon_g)$ which includes the Joule losses in the structure and radiative decay. The derivative in Eq. (13) is evaluated in the absence of gain $\varepsilon_g''=0$ and determines the linear rate of mode gain increase with material gain. For high values of material gain, the linear increase can break down. This is expected to happen when ε_g'' is not much smaller than ε_g'. In such a case, the evaluation of gain using the unperturbed modes in Eq. (9) will also be unreliable.

In the numerical evaluation of the derivative in Eq. (13), the increment of ε_g can in principle be either real or imaginary. This simply follows from the fact that the change in ω' caused by a change in ε_g' is the same as the change in ω'' caused by a change in ε_g''.

Definition (13) is similar to that for waveguides in which the confinement factor for a guided mode can be directly related to the derivative of the dispersion equation with respect to the dielectric constant of the gain material.[4] Certainly, the definition (13) can also be applied directly to waveguide-based resonators. However, in the case of waveguides, unlike subwavelength resonators, it is more convenient to separate the waveguiding properties and reflections from the facets.

The convenience of using Eq. (13) is in the absence of mode field and mode volume. Furthermore, the confinement factor can be calculated using the same numerical procedure as the resonant frequency. There are several approaches that can be used to calculate the resonant frequency. For example, one can calculate the scattering of waves by a resonant structure—the variation in the resonance with change in dielectric constant will give the confinement factor, according to Eq. (13). Below we will use a different approach—calculation of resonant frequencies using the characteristic equation for the resonator.

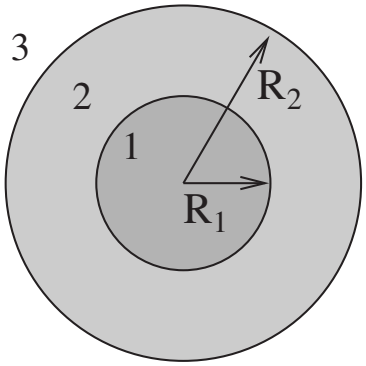

FIG. 1. Geometry of the investigated Ag rod (1) coated with gain material (2) and surrounded by matrix material (3).

IV. GAIN AND CONFINEMENT FACTOR FOR METAL RODS COATED WITH ACTIVE MATERIAL

Let us consider a subwavelength resonator as shown in Fig. 1 to demonstrate an approach of calculating the confinement factor based on Eq. (13). The resonator consists of a metal cylinder (material 1) coated with semiconductor (material 2) inside some matrix (material 3). There is no variation in the field along the axis of the cylinder, i.e., the problem is purely two-dimensional. Our numerical results will directly be relevant for long cylinders in which the radiation losses along the radial directions dominate. The approach in general is applicable to many other resonant structures, for example those with spherical geometry.

Since our practical interest in subwavelength structures, we consider the lowest resonant mode with the fields $\{\tilde{E}_\rho(\rho)\cos\varphi,\ \tilde{E}_\varphi(\rho)\sin\varphi,\ \tilde{H}_z(\rho)\sin\varphi\}e^{-i\omega t}$ where the frequency ω is complex. The solution of the Maxwell equations for H_z is

$$\tilde{H}_z = \begin{cases} AJ_1(k_1\rho), & \text{if } \rho < R_1, \\ BJ_1(k_2\rho) + CY_1(k_2\rho), & \text{if } R_1 < \rho < R_2, \\ DH_1(k_3\rho), & \text{if } \rho > R_2, \end{cases} \tag{14}$$

where J_1 and Y_1 are the Bessel functions of the first and second kind, respectively; $H_1=H_1^{(1)}$ is the Hankel function of the first kind (we omit the superscript for simplicity); A, B, C, and D are some constants; and $k_j=\omega\sqrt{\varepsilon_j}/c$, $j=1,2,3$ are the complex wave-numbers. Expressing $\tilde{E}_\varphi$ from Eq. (14) and matching the impedances at the outer interface give the condition which any mode must satisfy

$$f(\omega) = 0, \tag{15}$$

where

$$f(\omega) = \frac{\eta_3}{i}\frac{H_1'(k_3R_2)}{H_1(k_3R_2)} - Z_2\left(k_2R_1, k_2R_2, \frac{\eta_1}{i}\frac{J_1'(k_1R_1)}{J_1(k_1R_1)}\right),$$

$$Z_2(\varphi_1,\varphi_2,Z_1)=\frac{\eta_2-\eta_2 s_1(\varphi_1,\varphi_2)+iZ_1q_1(\varphi_1,\varphi_2)}{i\ -\eta_2 r_1(\varphi_1,\varphi_2)+iZ_1p_1(\varphi_1,\varphi_2)},$$

$$p_1(\varphi_1,\varphi_2)=J_1(\varphi_1)Y_1(\varphi_2)-J_1(\varphi_2)Y_1(\varphi_1),$$

$$q_1(\varphi_1,\varphi_2)=J_1(\varphi_1)Y_1'(\varphi_2)-J_1'(\varphi_2)Y_1(\varphi_1),$$

$$r_1(\varphi_1,\varphi_2)=J_1'(\varphi_1)Y_1(\varphi_2)-J_1(\varphi_2)Y_1'(\varphi_1),$$

$$s_1(\varphi_1,\varphi_2)=J_1'(\varphi_1)Y_1'(\varphi_2)-J_1'(\varphi_2)Y_1'(\varphi_1),$$

and $\eta_j=ck_j/(\omega\varepsilon_j)$.

The function $f(\omega)$ is the characteristic function for the resonator. Its zeros define the complex frequencies of the modes. The modes can be classified according to the values of the roots. For the investigated structure shown in Fig. 1, the characteristic equation does not have any solutions with purely real frequency. Real solution would denote a mode that does not decay in time such as the waveguiding modes of lossless structures. The characteristic Eq. (15) has only solutions with nonzero imaginary part. These solutions correspond to the modes that decay in time.

When solving Eq. (15) numerically, it is important to choose a proper values for the double-valued function $k_3(\omega)$. The sign for k_1 and k_2 can be chosen arbitrarily. For the mode decaying in time $\omega''<0$, the sign of k_3 must correspond to the energy flow from the cavity. This means taking Re $k_3>0$. The corresponding root has Im $k_3<0$ and gives a wave that grows exponentially as $\rho\to\infty$. This does not cause any physical contradiction since it describes an exponential decay of the energy in the resonator with time.

For the metal region, we use the experimentally measured[14] dielectric constant of Ag ($\varepsilon_1=\varepsilon_{\mathrm{Ag}}$) as interpolated in Ref. 15 for $\lambda>350$ nm (or $\hbar\omega<3.54$ eV)

$$\varepsilon_{\mathrm{Ag}}(\lambda)=a_0+a_1\lambda+a_2\lambda^2, \tag{16}$$

where the wavelength λ is measured in nanometers and the complex coefficients are $a_0=10.314+i1.0481$, $a_1=-0.026\,295-i0.003\,259$, and $a_2=-2.51\times10^{-5}+i5.3387\times10^{-6}$. The dielectric constant given by Eq. (16) is shown in Fig. 2. The numerical simulations used the usual root-finding subroutine.[16]

We start the analysis with the simple case of an Ag rod embedded in a semiconductor ($\varepsilon_2=\varepsilon_3=6$) without gain. Figure 3 shows the real and imaginary parts for the resonant frequency as well as the quality factor $Q=-\omega'/(2\omega'')$ for the resonator with ($\varepsilon_1''\neq0$) and without ($\varepsilon_1''=0$) the Joule loss of Ag. At $R_1\to0$, the long-wavelength (quasistatic) approximate resonant condition

$$\varepsilon_1(\omega')+\varepsilon_2\approx0 \tag{17}$$

and Eq. (16) give $\hbar\omega'\approx2.83$ eV, which is in perfect agreement with the numerical data presented on Fig. 3.

From Eq. (17) and Fig. 2, we can see that an increase in the background index ε_2 can shift the resonance to even lower energies. An increase in R_1, reduces ω'. This reduction is due to higher order terms in Eq. (15) beyond the simple long-wavelength resonance condition (17). The size-dependent shift in ω' is in the range of hundreds of millielectron volts even for the rods with sizes of $R\lesssim20$ nm. Such significant changes can be attributed to a relatively high background dielectric constant which leads to the break up of the long-wavelength approximation Eq. (17) in the structures of practical sizes.

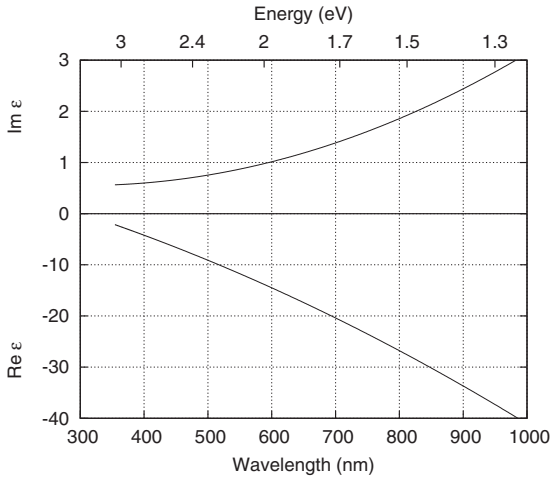

FIG. 2. Real and imaginary parts of the dielectric constant of bulk Ag as defined by Eq. (16). Note different vertical scales.

The radiative width for a lossless cylinder can be estimated using the asymptotic expansion of Eq. (15) around resonance (17)

$$\frac{\omega''}{\omega'}\approx-\frac{\pi}{2}\varepsilon_2^2\left(\frac{\omega R_1}{c}\right)^2\left(\omega'\frac{d\varepsilon_1'}{d\omega}\right)^{-1}. \tag{18}$$

The value for the derivative can be estimated at the point of resonance (17) using the dielectric constant (16) as

$$\omega\frac{\partial\varepsilon_1}{\partial\omega}\approx21.1. \tag{19}$$

The analytical result of Eqs. (18) and (19), which is shown in Fig. 4(b), agrees well with the numerical result for small R_1. At $R_1\to0$ the radiative decay vanishes and for Im $\varepsilon_1''=0$ the

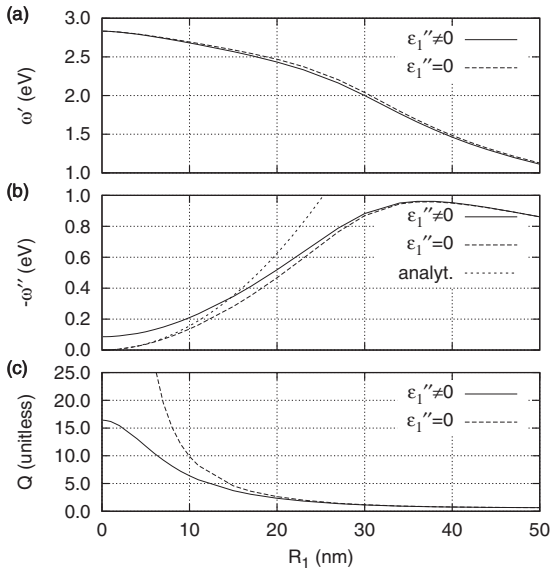

FIG. 3. Real (a), imaginary (b) parts of the resonant frequency, and Q-factor (c) as functions of R_1 for $\varepsilon_1=\varepsilon_{\mathrm{Ag}}$ and $\varepsilon_2=\varepsilon_3=6$. The analytical result shown in (b) corresponds to Eq. (18).

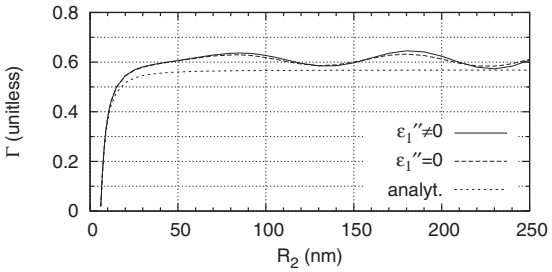

FIG. 4. Confinement factor as a function of R_2 for $\varepsilon_1=\varepsilon_{Ag}$, $\varepsilon_2=\varepsilon_3=6$, and $R_1=6$ nm. The analytical result is based on Eq. (21).

Q-factor goes to infinity. The losses due to ε_1'' can also be estimated analytically in the limit of $R_1\to 0$ using Eq. (17)

$$\frac{\omega''}{\omega'}=-\varepsilon_1''\left(\omega'\frac{d\varepsilon_1'}{d\omega}\right)^{-1}\approx -0.086\ \text{eV}, \tag{20}$$

which agrees with the numerical results in Fig. 3. The radiative damping for the cylinder exceeds the Joule loss for $R_1\gtrsim 5-10$ nm. This behavior is in contrast to that for spherical nanoparticles in which the radiative damping is smaller because it scales as $(\omega R/c)^3$, see Ref. 17. The dominance of Joule loss for small particles was also mentioned in the recent demonstration of a nanolaser.[3]

We now assume that the semiconductor region $\rho>R_1$ is divided into two parts: the part with $R_1<\rho<R_2$ provides gain while the part with $\rho>R_2$ does not. Both parts have the same $\varepsilon_2'=\varepsilon_3'=6$. This case allows one to use Eqs. (3)–(6) to calculate the confinement factor. To calculate the confinement factor analytically, we take the long-wavelength approximation for the cylinder, neglect Joule and radiative losses. Then using the mode profile, we can directly calculate the energy change per oscillation period due to the presence of small imaginary part in the region $R_1<\rho<R_2$. Normalizing this gain to that in a FP cavity we obtain the following result:

$$\Gamma=2\varepsilon_2\left(1-\frac{R_1^2}{R_2^2}\right)\left(\omega\frac{\partial\varepsilon_1}{\partial\omega}\right)^{-1}, \tag{21}$$

where the value for the derivative is given by Eq. (19). The confinement factors calculated numerically and analytically are plotted in Fig. 4. We can clearly see a good agreement between the analytical and numerical results for small R_2. In the long-wavelength approximation, Γ reaches the asymptotic value of

$$\Gamma_*\approx 0.57, \tag{22}$$

at $R_2/R_1\to\infty$, according to Eqs. (21) and (19). Furthermore, the same asymptotic value can be obtained directly by applying Eq. (13) to the long-wavelength resonance condition (17) without calculating any field distributions.

The asymptotic value [Eq. (22)] allows a simple physical interpretation. If one uses the plasma model for the metal

$$\varepsilon(\omega)=\varepsilon_0(1-\omega_p^2/\omega^2), \tag{23}$$

with ε_0 the background dielectric constant and ω_p the plasma frequency, the asymptotic value becomes $\Gamma_*=\varepsilon_2/(\varepsilon_0+\varepsilon_2)$. Thus, for $\varepsilon_0=\varepsilon_2=1$, one obtains $\Gamma_*=1/2$. The later value can be explained by the fact that the energy is exchanged periodically between the kinetic energy of the electrons and the electric field. Only half of the electric energy is outside of the metal and, therefore, the time-averaged electric field in the gain region is only a quarter of the total energy. Compared to the one-half value for a FP resonator with the same gain medium, we naturally obtain $\Gamma_*=1/2$. The presence of the background dielectric constant for Ag as described by Eq. (16) and $\varepsilon_2\neq 1$, changes this value to $\Gamma_*\approx 0.57$. In general, we can conclude that the high fraction of energy in the kinetic motion of electrons and in the electric field inside the metal are disadvantageous to obtaining high Γ, according to Eq. (9).

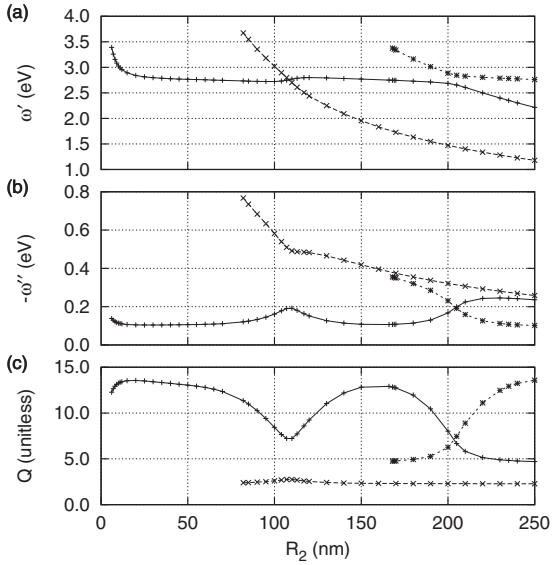

FIG. 5. Real (a), imaginary (b) parts of the resonant frequency, and Q-factor (c) as functions of R_2 for $\varepsilon_1=\varepsilon_{Ag}$, $\varepsilon_2=6$, $\varepsilon_3=2.4$, and $R_1=6$ nm. Different curves describe different resonances.

We need to comment on the difference between the analytical and numerical results in Fig. 4 for $R_2\gtrsim 20$ nm. The analytical model is based on the long-wavelength approximation while the numerical results are on rigorous solution (14) of the Maxwell equations. So it is quite natural that there is a difference for large sizes of the gain region. However, the oscillations in the confinement factor do not seem to be consistent with Eq. (9) that predicts a monotonic dependence of Γ with the size of the gain region. This can perhaps be explained as follows. The presence of small perturbation in the dielectric constant, as required for calculating the derivative (13), in region 2 causes a reflection of the field from the interface between regions 2 and 3. This reflection changes the field distribution and modifies the shape of the mode, that is outside of the approximation of Eq. (9). One, therefore, obtains oscillations as a consequence of the interference effects. We also have to point out that the amplitude of the oscillations in Γ grows weakly with R_2. This growth, however, becomes noticeable for R_2 larger than that used for Fig. 4 and can become an issue only for very thick active region that may require a different treatment.

We now turn to the investigation of the layered structure with gain region. We fix $R_1=6$ nm and assume that $\varepsilon_2=6$ (semiconductor) and $\varepsilon_3=2.4$ (polymer). Figure 5 shows the properties of several lowest modes. At $R_2\to R_1$, ω' corre-

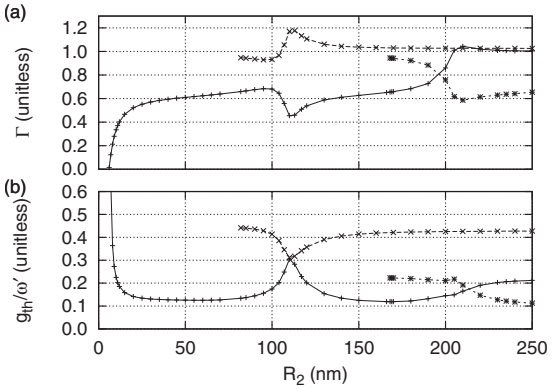

FIG. 6. Confinement factor (a) and threshold gain normalized to the real part of the resonant frequency (b) for the same structure as Fig. 5.

sponds to that of an Ag rod in matrix with $\varepsilon_3=2.4$. An increase in R_2 causes an initially rapid decrease in ω' due to a higher value of ε_2 as compared to ε_3, see Eq. (17). When the size of the coating becomes comparable to the wavelength, the reflection from the boundary gives rise to anticrossing behavior of various modes. The anticrossing behavior, however, does not seem to be clearly manifested on Fig. 5(a) at around $R_2 \sim 110$ nm. This is most likely related to the fact that the modes have quite different imaginary parts of the frequencies so the crossing of their real parts can be possible.

In the interval 20 nm$<R_2<$80 nm, the resonant position and damping change relatively weakly. The Q-factor is about 12–14 for $R_2<80$ nm. This is comparable to the estimated $Q\approx 14$ for the operational nanoparticle lasers in Ref. 3. However, unlike nanoparticles, the losses in the nanorod are mostly radiative. The drop of the Q-factor at $R_2 \sim 110$ nm can be explained by the interference effects due to reflection from the interface between media 2 and 3 which have different dielectric constants.

The confinement factor calculated using Eq. (13) for the resonator is shown in Fig. 6(a). The confinement factor initially increases from zero at $R_2 \to R_1$. This corresponds to the limit of vanishing thickness of active region. The confinement factor shows some rapid variation in the region around $R_2 \approx 110$ nm due to the interaction between the modes.

The threshold gain shown in Fig. 6(b) is calculated using $g_{th}=2\omega''/\Gamma$ where ω'' is due to radiative and Joule losses. As expected, for very thin active layers the threshold gain is very large. In the large interval 20 nm$<R_2<$80 nm, the threshold gain (normalized to the frequency) remains practically constant and $g_{th}/\omega' \lesssim 0.15$. We note $g_0/\omega'=-\varepsilon_2''/\varepsilon_2'$, according to Eq. (13). This value corresponds to the plane wave gain $g_{pw}=(g_0/\omega')(\omega'\sqrt{\varepsilon'}/c)\approx 5.1\times 10^4$ cm^{-1} at $\omega'=2.75$ eV. This value is a factor of $\sim$3 larger than typically ($\sim 1-2\times 10^4$ cm^{-1}) achievable in semiconductor materials. Our estimates, however, rely on losses in Ag based on the experimental data from Ref. 14. According to recent results,[18] there is a large variation in $\varepsilon_{\mathrm{Ag}}$ depending on specific samples and $\varepsilon''_{\mathrm{Ag}}$ can be a factor of 2–3 smaller that of Eq. (16). Therefore, one can conclude that the compensation of losses and lasing might be achievable in coated Ag rods.

V. CONCLUSION

To conclude, we discussed the confinement factor for a resonator and demonstrated an approach to calculate it as a derivative of the resonant frequency with respect to the dielectric constant in the gain region. This avoids uncertainties related to the calculation of the actual field distribution and defining the cavity size. In practice, this confinement factor allows one to calculate directly the required material gain to achieve lasing. This approach is naturally applicable both to subwavelength and usual resonators.

Using our definition, we analyzed the possibility of lasing in a simple structure—Ag rod coated with active material. To find the resonances, we numerically calculated the complex roots of the characteristic equation using the field representation in the cylindrical geometry. In more complicated structures, various discretization techniques applied to the Maxwell equations can produce a discretized equivalent of the characteristic equation without limiting the applicability of our approach. This makes it suitable for various other resonant subwavelength structures of interest such as metal nanoparticles of complicated shapes, nanoshells, bow-ties. Furthermore, one can calculate scattering by a resonant structure (for example, a photonic crystal cavity) to determine the change in resonant frequencies and, therefore, the confinement factor. Although we analyzed the case of the uniform active region, nonuniform regions can be treated using the similar approach and defining a spatially varying confinement function. Finally, our specific analysis of a coated Ag rod structure provided specific (and quite severe) requirements for the threshold gain in order to compensate radiative and Joule losses.

[1] D. J. Bergman and M. Stockman, Phys. Rev. Lett. **90**, 027402 (2003).
[2] N. M. Lawandy, Appl. Phys. Lett. **85**, 5040 (2004).
[3] M. A. Noginov, G. Zhu, A. M. Belgrave, R. Bakker, V. M. Shalaev, E. E. Narimanov, S. Stout, E. Herz, T. Suteewong, and U. Wiesner, Nature (London) **460**, 1110 (2009).
[4] A. V. Maslov and C. Z. Ning, in *Nitride Semiconductor Devices: Principles and Simulation*, edited by J. Piprek (Wiley-VCH, Weinheim, 2007).
[5] R. Yan, D. Gargas, and P. Yang, Nat. Photonics **3**, 569 (2009).
[6] R. Ikkawi, N. Amos, A. Krichevsky, R. Chomko, D. Litvinov, and S. Khizroev, Appl. Phys. Lett. **91**, 153115 (2007).
[7] S. W. Chang and S. L. Chuang, IEEE J. Quantum Electron. **45**, 1014 (2009).
[8] A. V. Maslov and C. Z. Ning, IEEE J. Quantum Electron. **40**, 1389 (2004).
[9] D. B. Li and C. Z. Ning, Phys. Rev. B **80**, 153304 (2009).
[10] D. B. Li and C. Z. Ning, Appl. Phys. Lett. **96**, 181109 (2010).
[11] Y. Z. Huang, Z. Pan, and R. H. Wu, J. Appl. Phys. **79**, 3827 (1996).
[12] T. D. Visser, H. Blok, B. Demeulenaere, and D. Lenstra, IEEE J. Quantum Electron. **33**, 1763 (1997).
[13] J. A. Gordon and R. W. Ziolkowski, Opt. Express **15**, 2622 (2007).
[14] E. Palik and G. Ghosh, *Handbook of Optical Constants of Solids II* (Academic, New York, 1991).
[15] J. A. Dionne, L. A. Swatlock, H. A. Atwater, and A. Polman, Phys. Rev. B **72**, 075405 (2005).
[16] GNU Scientific Library (GSL), http://www.gnu.org/software/gsl/
[17] V. B. Gil'denburg, Y. M. Zhidko, I. G. Kondrat'ev, and M. A. Miller, Radiophys. Quantum Electron. **10**, 761 (1967) [Izv. Vyssh. Uchebn. Zaved., Radiofiz. **10**. 1358 (1967)].
[18] V. P. Drachev, U. K. Chettiar, A. V. Kildishev, H. K. Yuan, W. Cai, and V. M. Shalaev, Opt. Express **16**, 1186 (2008).